Recoil Range Measurements of Reactions Induced in Ni^{58} with 46- to 68-MeV Helium Ions*

MARSHALL BLANN AND ALAN EWART
Department of Chemistry, The University of Rochester, Rochester, New York
(Received 3 January 1964)

Ranges in Ni^{58} are reported for Ni^{56}, Ni^{57}, Co^{55}, Co^{56}, Co^{57}, and Co^{58} recoil ions resulting from the bombardment of Ni^{58} with 46- to 68-MeV helium ions. The thick target-thick catcher method was used to obtain average recoil ranges in the beam direction. Measured ranges have been compared with theoretical range predictions, calculated assuming full momentum transfer from the incident helium ions to the recoil ions. Theoretical range curves were corrected for the influence of α particle and nucleon evaporation. Experimental ranges measured from reaction thresholds to excitation function peaks agree with the corrected theoretical curves to within 10%. Recoil ranges for Co^{57} and Ni^{57} are shown to have predominate contributions from a low-momentum-transfer process in the energy range corresponding to the high-energy tail of the excitation functions. At higher energies the ranges and excitation functions are shown to increase, consistent with contributions from the onset of Ni^{58} (α,5 nucleon) compound-nucleus reactions. Recoil ranges for Co^{55}, Co^{56}, and Co^{58} are consistent with full momentum transfer over the entire energy range studied, including those ranges corresponding to the high-energy tail of the Co^{56} excitation function. Recoil ranges for Ni^{56} are consistent with full momentum transfer up to the peak of the excitation function, after which the range decreases sharply as a competing low momentum-transfer reaction becomes predominant. We discuss the details of the reaction mechanism responsible for the high-energy tails of the Ni^{57}, Co^{57}, and Ni^{56} excitation functions. In the case of the tail of the excitation-function for the formation of Ni^{56} we present evidence that the interaction is between the incident helium ion and one or two neutrons, rather than an (α,α') inelastic scattering followed by nucleon evaporation. We conclude that we cannot differentiate between these two mechanisms in the case of the reactions forming Ni^{57} and Co^{57}.

I. INTRODUCTION

MANY measurements of excitation functions have been undertaken to provide data to test the statistical theory[1–4] of nuclear reactions. Some of the reactions to be discussed in this work [(α,αn), (α,αp), (α,αpn), and (α,$\alpha 2n$) reactions of Ni^{58}] have been studied extensively by several groups.[5–8] There are disagreements between the experimental excitation functions for these reactions and the predictions of the statistical theory in its most commonly applied form.[9–11] Specifically, the experimentally measured yield ratios of Ni^{57}/Co^{57} and Ni^{56}/Co^{56} are very much lower than predicted by the statistical theory, and the high-energy tails of the excitation functions are not predicted by theory. The discrepancies could arise either from significant direct-reaction contributions[5] (which would make a comparison with statistical theory invalid) or from a failure of the statistical theory in the form in which it has been applied (or to a combination of these). This work was undertaken in an effort to differentiate between the possible explanations, to determine the reaction mechanisms in general, and, in particular, to see where a comparison with the statistical theory is valid (i.e., where reactions appear to be proceeding by a compound-nucleus mechanism). In a subsequent work, the statistical theory will be applied to those reactions shown to proceed by a compound nucleus mechanism.[8]

From excitation functions alone, one may only speculate as to the mechanism of a reaction. Measurements giving more specific information include angular distributions, angular correlations, and recoil-range measurements.

Alpha-particle angular distributions resulting from helium-ion bombardment of Fe^{56} and $Cu^{63,65}$ with helium ions of 21 to 47 MeV are symmetric about 90° c.m. and have energy distributions consistent with evaporation spectra.[12–14] These data imply that the preponderance of (α,α') reactions in this region do proceed by a compound-nucleus mechanism, but they do not give specific information on the mechanism responsible for the high-energy tails of the excitation functions. This is because the cross section in the tail region of excitation functions may be only 1–10% of the total α-emitting cross section at a given bombarding energy. Thus, if the angular distributions of reactions leading to excitation-function tails were asymmetric about 90°, the observation of this asymmetry might be

*This work is supported by the U. S. Atomic Energy Commission.

[1] H. A. Bethe, Rev. Mod. Phys. **9**, 69 (1937).
[2] V. F. Weisskopf, Phys. Rev. **52**, 295 (1937).
[3] S. Wolfenstein, Phys. Rev. **82**, 690 (1951).
[4] T. Ericson and V. Strutinski, Nucl. Phys. **8**, 284 (1958).
[5] F. S. Houck and J. M. Miller, Phys. Rev. **123**, 231 (1961).
[6] S. Tanaka, J. Phys. Soc. Japan **15**, 2159 (1961).
[7] M. Blann and G. Merkel, Nucl. Phys. (to be published).
[8] M. Blann and G. Merkel (to be published).
[9] I. Dostrovsky, Z. Fraenkel, and G. Friedlander, Phys. Rev. **116**, 683 (1960).
[10] E. A. Bryant, D. R. F. Cochran, and J. D. Knight, Phys. Rev. **130**, 1512 (1963).
[11] M. Blann and G. Merkel, Phys. Rev. **131**, 764 (1963).
[12] H. W. Fulbright, N. O. Lassen, and N. O. Roy Poulson, Kgl. Danske Videnskab. Selskab, Mat.-Fys. Medd. **31**, No. 10 (1959).
[13] J. Benveniste, G. Merkel, and A. Mitchell, Bull. Am. Phys. Soc. **7**, 454 (1962).
[14] G. Merkel, University of California Lawrence Radiation Laboratory Report UCRL 9898, 1962 (unpublished).

lost due to the preponderant contributions of other α-emitting reactions. Angular correlation measurements would suffer similar difficulties, due to the competitive behavior of reactions proceeding by the compound-nucleus mechanism.

The measurement of recoil ranges of residual nuclides leaves no ambiguity as to the reaction being investigated. The recoil range is, as will be discussed, quite sensitive to deviations from symmetry about 90° c.m. of the emitted alpha particle. In this work we report measured mean recoil ranges in the beam direction for the $(\alpha,\alpha n)$, $(\alpha,\alpha p)$, $(\alpha,\alpha pn)$, $(\alpha,\alpha 2np)$, $(\alpha,\alpha 2n)$, and $(\alpha,3pn)$ reactions induced in Ni^{58}.

We will first discuss the theoretical predictions of recoil ranges in nickel for the nuclides of interest. We will discuss the corrections to the predicted ranges due to changes in momentum and direction of the recoil products resulting from particle evaporation, yielding theoretical range-energy relations for the recoil nuclei of interest. We will then present and compare the experimental ranges with the values calculated assuming a compound-nucleus mechanism, and discuss the implications of these results with respect to reaction mechanisms.

II. EXPERIMENTAL PROCEDURES

A. Targets and Catcher Foils

Targets were prepared by electroplating 99.95% enriched Ni^{58} onto 0.2-mil gold foils. Each gold cathode was individually weighed and measured prior to use to determine its thickness; thicknesses varied between 9.3 and 10.0 mg/cm². The plating chimneys used gave circular plates of 1.90 cm diam. The target thicknesses varied between 4.07 and 9.52 mg/cm². The catcher-degrader foils used were 99.5% pure aluminum, 2.02 mg/cm² thick.

Two sets of targets were bombarded. Each stack consisted of ten targets of Ni^{58} on gold, each followed by an aluminum catcher foil. Additionally, each stack had nine targets of Fe^{56} on gold followed by aluminum catcher foils. The Fe^{56} targets were part of a separate experiment being run concurrently; the results of this experiment will not be discussed in detail in this work. Targets were arranged with the nickel on the downstream side of the gold foils with respect to the beam; aluminum catcher foils followed the nickel. Each complete target stack was wrapped in a single layer of 5.0-mg/cm² aluminum foil for ease of handling.

B. Bombardments

Bombardments were performed on the University of California Lawrence Radiation Laboratory 88-in. spiral ridge cyclotron. The two target stacks were each bombarded for approximately 15 min in a 0° beam port 33 ft from the accelerator. A $\frac{1}{2}$-in.-diam graphite collimator was placed 12 in. in front of the target holder. The integrated beam on the two runs was 0.11 and 0.30 μA-h, respectively.

The energy of the incident helium-ion beam is estimated to be 69±1 MeV. This estimate is based on the extraction radius and cyclotron frequency. The calculated values were found to give good agreement with energy determinations based on aluminum range measurements.[15]

C. Chemistry

Targets and their respective catcher foils were dissolved separately in 8*M* HCl solutions to which Co and Fe carriers, and Mn and Na holdback carriers had been added. Additionally, Ni carrier was added to the solutions containing the catcher foils. The resulting solutions were passed through Dowex-1 anion-exchange columns, which were rinsed with equal volumes of 8*M* HCl. Cobalt and iron complexes were retained on the resin, all other ions were in the eluant.[16] Cobalt was removed from the column with 4*M* HCl, and was precipitated as $K_3Co(No_2)_6\cdot H_2O$. Yields were subsequently determined colorimetrically.

Five mg of Co carrier was added to each Ni sample eluted from the columns. After five days the solutions were again separated by ion exchange as in the initial separation above. In this time 90% of the Ni^{57} had decayed to Co^{57}, simplifying spectroscopy for Ni^{56} γ rays. The eluted solution containing Ni, Mn, Al, and Na was made basic with an excess of NaOH, precipitating hydroxides of Ni and Mn. The hydroxides were dissolved in a minimum volume of 6*N* HCl. The resulting solution was made alkaline with an excess of NH_4OH. Several drops of 3% H_2O_2 were added to the ammoniacal solution to oxidize manganese to the +4 oxidation state, in which form its hydroxide is insoluble in ammoniacal solution. The resulting $Ni(NH_3)_4^{++}$ solution was diluted with distilled water, and excess dimethylglyoxime was added to precipitate Ni. Separation of Ni and Mn was necessary because of the similarity of half-lives and γ-ray spectra of Ni^{56} and Mn^{52}; tracer amounts of Mn would coprecipitate with nickel-dimethylglyoxime if no prior separation had been performed. Nickel yields were subsequently determined colorimetrically.

D. Recoil Ranges

In this section we discuss the problems peculiar to the range determination of each isotope investigated. We attempt to make an estimate of the accuracy of each set of determinations based on possible errors in chemical yields, target thickness, and most important, counting statistics. In general, branching ratios, abun-

[15] B. G. Harvey (private communication).

[16] B. G. Harvey, *Introduction to Nuclear Physics and Chemistry* (Prentice-Hall, Inc., Englewood Cliffs, New Jersey, 1962), Chap. 15, p. 313.

dances, and detector efficiencies do not enter into a consideration of the accuracy, since ratios of activities in catcher foil and targets are required, and the above mentioned efficiency factors cancel. Where such corrections were required, we mention them briefly and consider them in the estimate of error quoted. The precision of the measured ranges appears in general to be far better than the errors we quote; a few points, however, seem to have errors far outside those estimated. The radiation observed for each isotope studied is summarized in Table I, with additional pertinent decay

TABLE I. Decay characteristics of isotopes studied in this work.[a]

Nuclide	Type of radiation observed	Energy of radiation observed (MeV)	Assumed half-life	Detection apparatus
Ni^{56}	γ	0.164	6.1 day[b]	3-×3-in. NaI crystal
Ni^{57}	β^+	continuous	36.0 h	End-window proportional counter
Co^{55}	β^+	continuous	18.2 h	End-window proportional counter
Co^{56}	γ	1.26	77 day	3-×3-in. NaI crystal
Co^{57}	γ	0.120	270 day	1½-×1-in. NaI crystal
Co^{58}	γ	0.810	71 day[c]	3-×3-in. NaI crystal

[a] D. Strominger, J. M. Hollander, and G. T. Seaborg, Rev. Mod. Phys. **30**, 585 (1958), unless otherwise referenced.
[b] D. O. Wells, S. L. Blatt, and W. E. Meyerhoff, Phys. Rev. **130**, 1961 (1963).
[c] The area under the 0.810-MeV photopeak represented the yield of Co^{56} and Co^{58}. The fraction of the peak due to Co^{56} was calculated from the area of the 1.26 MeV photopeak (assuming 0.70–1.26-MeV transitions per 0.845-MeV transition) and subtracted from the total 0.810-MeV photopeak area to obtain the Co^{58} contribution.

data. The measured mean projected recoil ranges [calculated with Eq. (1) of the following section] are listed in Table II.

1. Ni^{56}

Three determinations were made of the 0.160 MeV γ-ray photopeak area for each Ni sample (targets and catchers). All areas were extrapolated to a common time by use of the Ni^{56} half-life quoted in Table I, and averaged for each sample. The three counts were taken at periods of one to four weeks after the bombardment. Photopeak area precision for the target foil samples was 3%, and for the catcher foils approximately 7%, indicating that the measured photopeaks decayed with the proper half-life. We estimate the Ni^{56} ranges to be accurate to ±10%.

2. Ni^{57}

Nickel-57 ranges were calculated from the relative activities of the 36-h β^+ radiation, extrapolated to a common time. All samples from the catcher foils were of the same thickness within 5%, and so all had the same counting efficiency. The samples from the targets varied widely in sample thickness (see Table II, column

TABLE II. Mean projected recoil ranges in Ni^{58} of reaction products produced by helium ion bombardment of Ni^{58}.

Average helium ion energy in target (MeV)[a]	Target thickness (mg/cm²)	Range in Ni^{58} (mg/cm²) Ni^{56}	Ni^{57}	Co^{55}	Co^{56}	Co^{57}	Co^{58}
67.8	7.32	0.48	0.58	0.76	0.94	0.60	b
67.1	5.56	0.49	0.35	0.79	0.74	0.65	0.77
65.7	8.40	0.38	0.25	0.80	0.84	0.61	b
64.9	8.15	0.54	0.32	0.85	0.79	0.63	0.80
63.3	7.36	0.55	0.33	0.94	1.05	0.74	b
62.8	9.52	0.56	0.30	0.79	0.86	0.57	0.80
61.0	6.68	0.56	0.29	0.78	0.83	0.56	b
60.6	4.67	0.60	0.29	0.73	0.80	0.54	0.77
59.1	7.10	0.62	0.30	0.74	0.68	0.52	b
58.4	7.26	0.59	0.32	0.71	0.73	0.47	0.75
56.9	4.43	0.64	0.26	0.71	0.74	0.49	b
56.1	6.62	0.56	0.25	0.76	0.79	0.43	0.74
54.7	6.69	0.67	0.29	0.71	0.75	0.50	b
53.8	5.65	0.69	0.28	0.71	0.72	0.48	0.68
52.3	4.07	0.69	0.29	0.69	0.75	0.46	b
51.2	6.68	0.70	0.35	0.74	0.74	0.50	0.75
49.8	6.28	0.71	0.34	0.66	0.67	0.53	b
48.7	5.12	0.71	0.37	0.74	0.64	0.54	0.68
47.4	6.44	0.66	0.39	0.65	0.61	0.57	b
46.1	8.42	0.68	0.40	0.61	0.69	0.59	0.63

[a] Calculated with the range-energy values of W. H. Barkas, University of California Lawrence Radiation Laboratory Report UCRL-10292, 1962 (unpublished).
[b] Not calculated due to large statistical uncertainties.

2), requiring efficiency corrections to thicknesses comparable to the catcher foil samples. These corrections were obtained from calibration curves of the end window proportional counter used[17]; the calibration was by the method of Bayhurst and Prestwood.[18] We estimate the measured ranges to be accurate to ±10%.

3. Co^{55}

Ranges of Co^{55} recoils were determined by monitoring the β^+ radiation with an end-window proportional counter. All samples were of comparable thickness; activity levels were very satisfactory. We estimate these ranges to be accurate to ±7%. Gamma pulse-height analysis was performed on all cobalt samples from catcher foils within 20 h of bombardment time. No evidence of Na^{24} activity was found, which indicated the efficiency of the Na holdback carrier used in the chemical separations.

4. Co^{56}

Gamma-ray spectroscopy was used in obtaining Co^{56} activities in target and catcher foils. The main problem in these measurements was the low activity of some of the catcher foil samples with respect to background. Because of this difficulty we estimate that the Co^{56} ranges quoted are accurate only to ±15%.

[17] M. Blann, University of California Lawrence Radiation Laboratory Report UCRL 9190, 1960, Appendix B (unpublished).
[18] B. P. Bayhurst and R. J. Prestwood, Nucleonics **17**, 82 (1959).

5. Co^{57}

The 0.120 MeV γ-ray activity due to Co^{57} decay was determined one month after bombardment. A pulse-height analyzer was used with a $1\frac{1}{2}$-$\times$1-in. NaI crystal. Counting statistics were satisfactory for all samples. We estimate these ranges to be accurate to $\pm 8\%$.

6. Co^{58}

Cobalt-58 activities were measured by γ-ray spectroscopy of the 0.810-MeV photopeak. It was necessary to correct the area under the 0.810-MeV photopeak for contributions from Co^{56}. This was done by calculating the 0.810-MeV γ-ray activity due to Co^{56} based on the area under the 1.26-MeV Co^{56} γ-ray photopeak. The crystal efficiency curves of Heath were used for this purpose.[19] Coincidence corrections were applied. This procedure often resulted in taking differences in numbers differing by as little as 25%. For this reason we have not calculated Co^{58} ranges for the first bombardment (0.11-μ A–h beam). For the second set of foils which showed higher disintegration rates we estimate an accuracy of $\pm 15\%$ for the Co^{58} ranges listed in Table II.

III. RANGE-ENERGY RELATIONSHIPS

A. General Discussion

As stated in the introduction, we have measured average recoil ranges in the beam direction $\bar{R}_x$ for reaction products of interest. We have used the thick-target thick-catcher method, where both the targets and catcher foils were several times thicker than the maximum recoil ranges encountered. Under these experimental conditions the relationship between the target thickness T, the experimentally measured fraction of the total activity in the catcher foil f, and the mean range $\bar{R}_x$, is[20]

$$\bar{R}_x = fT. \tag{1}$$

We wish to compare the experimentally measured ranges with theoretical ranges calculated assuming full momentum transfer in the initial reaction, i.e.,

$$E_R = E_\alpha[M_\alpha/(M_T+M_\alpha)][M_R/(M_T+M_\alpha)], \tag{2}$$

where E_R represents the recoil energy of the compound nucleus resulting from helium ions of kinetic energy E_α and mass M_α, interacting with a target of mass M_T to give a final reaction product of mass M_R. The calculation of the range values is complicated by two factors. First, the velocities of the recoils encountered in this work are such that electronic and nuclear stopping are both significant; neither may be ignored in calculating theoretical ranges. Secondly, the masses of recoiling atoms and stopping medium are nearly equal, so that corrections for scattering are not trivial.

B. Theoretical Ranges

Theoretical range calculations fulfilling the needs of this work have recently been performed by Lindhard, Scharff, and Schiott (hereafter referred to as LSS).[21] Their results are presented as a universal set of range-energy curves expressed by the dimensionless variables ρ, ϵ, where

$$\rho = \frac{(0.8853)^2(RNM_2)4\pi a_0^2 M_1}{(M_1+M_2)^2(Z_1^{2/3}+Z_2^{2/3})} \tag{3}$$

and

$$\epsilon = \frac{0.8853 E_R M_2}{Z_1 Z_2 e^2 (M_1+M_2)(Z_1^{2/3}+Z_2^{2/3})^{1/2}}, \tag{4}$$

and where the subscripts 1 and 2 denote the recoil ion and stopping medium, respectively. R represents the range in cm, N the number of atoms of stopping medium per cm^3, and E_R the recoil-ion kinetic energy. The symbols a_0, M, and Z have their customary denotation. When electronic stopping as well as nuclear stopping is considered, a family of curves in the $\rho-\epsilon$ plane results, where

$$\left(\frac{d\epsilon}{d\rho}\right)_{\text{electronic}} = kE_R^{1/2} \tag{5}$$

and

$$k = \frac{0.0793 Z_1^{2/3} Z_2^{1/2} (A_1+A_2)^{3/2}}{(Z_1^{2/3}+Z_2^{2/3})^{3/4} A_1^{3/2} A_2^{1/2}}. \tag{6}$$

The theoretical curves shown in Fig. 1 were calculated from the $\rho-\epsilon$ curves of LSS, interpolated for $k=0.16$, for a recoiling ion of $Z=27$, $A=56$ in Ni^{58}. Corrections for scattering (calculated by LSS) were applied to get ranges in the beam direction. The maximum deviation between the range values calculated for any isotope studied in this work and the average value ($A=56$, $Z=27$) used above does not exceed 3% [see Eqs. (2)–(6)]. The abscissa of Fig. 1 gives the incident helium-ion energy; the recoil energy may be calculated with Eq. (2) using $M_R=56$. For a 100-MeV helium ion, the recoil energy would be 5.8 MeV. The range-momentum curve has also been shown in Fig. 1: note that the range is not solely proportional to energy or to momentum.

The theoretical range curve of Fig. 1. was calculated, as stated above, for a mass-56 recoil ion which had received full momentum transfer from the incident helium-ion beam. The ranges measured experimentally in this work are (with the exception of Co^{58} recoils) for recoils which have emitted an α particle and one to

[19] R. L. Heath, Atomic Energy Commission Research and Development Report IDO—16408, 1957 (unpublished).

[20] L. Winsberg and J. M. Alexander, Phys. Rev. **121**, 518 (1961).

[21] J. Lindhard, M. Scharff, and H. E. Schiott, Kgl. Danske Videnskab. Selskab, Mat.-Fys. Medd. **33**, No. 14 (1963).

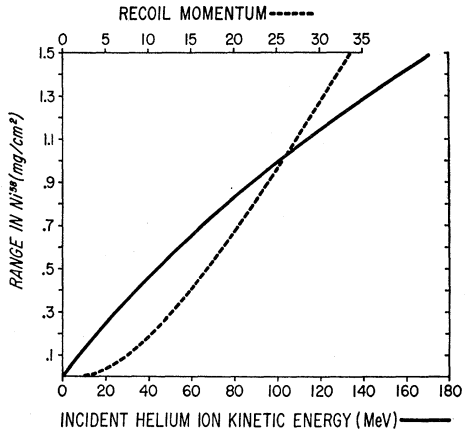

FIG. 1. Range-energy and range-momentum curves for Co^{56} recoil ions in Ni^{58} calculated from the curves of LSS (Ref. 21). The energy abscissas is calculated as the incident helium ion kinetic energy on a mass 58 target, assuming full momentum transfer to the recoil of mass 56. The momentum (upper) abscissas is calibrated in units of $(2\times56\times E_R)^{1/2}$, where E_R is the recoil energy in MeV.

three nucleons before traversing any significant part of their range. This particle emission may profoundly affect the recoil ranges. Before comparing the experimental range values with the theoretical range curve of Fig. 1, appropriate corrections must either be applied to the experimentally measured ranges or to the theoretical-range curve. Our goal is to determine where experimental recoil values correspond to reactions characterized by full momentum transfer in the initial interaction, followed by particle evaporation which is symmetric about 90° c.m. We therefore choose to construct a theoretical-range curve (as a function of incident helium-ion energy) corresponding to such a situation. We will then compare the experimentally determined ranges with these theoretical predictions to determine where such a correspondence exists. In the remaining paragraphs of this section we shall discuss these corrections to the range-energy curve of Fig. 1, and construct corrected range-energy curves (Fig. 2). We shall show that the corrections to the range-energy curve are greater for α emission than for nucleon emission, and that the range is fairly insensitive to α particle anisotropy and energy, so long as the emitted α particle is symmetric with respect to 90° c.m. We shall also show that the mean recoil range is quite sensitive to a forward peaking of the emitted α particle.

1. *Range Corrections for Alpha-Particle Emission*

We wish to recalculate the range energy curve on the assumption that the recoiling nuclei each evaporate an α particle before traversing their range. Evaporation calculations which consider multiple-particle emission predict an average α energy of $\approx$12 MeV for nuclei of mass 60 at initial excitations of 48 to 70 MeV.[22] We shall use this average value in our calculations. Use of the full spectrum does not introduce a significant change into the final results, as will be discussed in the following paragraph.

An example of the influence of α emission on recoil energy might emphasize the importance of the correction. If, for example, a recoiling ion of 4.5-MeV kinetic energy emitted a 12-MeV α particle in the forward direction, the resultant recoil energy would be 1.4 MeV; if the α were emitted in the backward direction, the resultant recoil energy would be 9.3 MeV. If the emitted α-particle energy were 8 MeV, the resultant recoil energies would be 1.8 and 8.3 MeV, respectively, and for a 16-MeV α, 1.3 and 9.6 MeV. The change of the average range $\bar{R}_x$ for the 8- or 16-MeV α emission is less than 1.5% of the value calculated for a 12-MeV α.

In the preceding paragraph it was shown that the use of an average α-particle energy in place of the complete spectrum is a good approximation. The next consideration should be the angular distribution of the emitted α particle. The extremes one might consider range from an isotropic distribution to one in which all α particles are emitted in the forward and backward directions along the beam axis. Experimental measurements of alpha-particle angular distributions show that there is considerable anisotropy in this mass region with 27- and 48-MeV incident helium ions.[13] Since the incident helium ions of this work had energies of 46 to 68 MeV, we might also expect a great deal of anisotropy in these α-particle angular distributions. We have, therefore, calculated one range curve with the extreme assumption that half the alphas are emitted at 0°, and half at 180°. This curve is presented in Fig. 2.

We also wish to consider the case of isotropic α emission. We have calculated the theoretical-range curve for isotropic (c.m.) emission of 12-MeV alphas, with the relationship

$$\bar{R}_x=\int_{0^\circ}^{180^\circ} R(P_x')\cos\phi\,\sin\theta d\theta \Big/ \int_{0^\circ}^{180^\circ}\sin\theta d\theta, \quad (7)$$

where $R(P_x')$ represents the range of the recoil of momentum P_x' along the $\mathbf{P}_x'$ momentum vector, and the other quantities are defined in the momentum vector diagram of Fig. 3. The integration was actually done graphically due to the inconvenient functional dependence of range and momentum in the region of interest. The result of this calculation is shown in Fig. 2. It may be seen that this result does not differ appreciably from the 0°–180° range curve calculated above. A $1/\sin\theta$ angular distribution lies between the two previously calculated values, and since it differs so little from the case of isotropic emission this curve has not been shown in Fig. 2.

2. *Range Corrections Due to Nucleon Emission*

Evaporation calculations predict average neutron and proton kinetic energies of 3.5 and 7.5 MeV, respec-

[22] M. Blann, Phys. Rev. **133**, B707 (1964).

tively, for nuclei considered in this work.[22] The relative average momenta due to α, p, and n emission are therefore 1.0:0.38:0.27. Since as many as three nucleons are emitted in addition to the α in the reactions studied in this work, it is desirable to consider the influence of nucleon emission on recoil range. We note in Fig. 2 that the range calculated assuming a forward-backward α angular distribution is within 3% of the range calculated for an isotropic distribution for incident helium ions between 45 and 70 MeV. We have therefore, for simplicity, assumed a forward-backward angular distribution for nucleon emission in order to get an estimate of the effect of nucleon evaporation on mean recoil range.

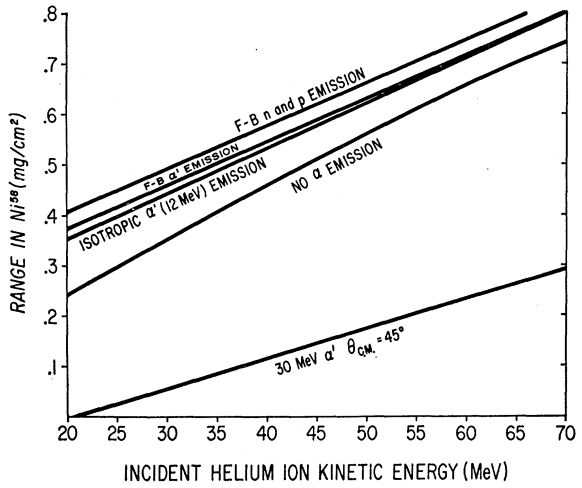

FIG. 2. Theoretical range-energy curves pertinent to this work. The curve designated "no α emission" is the curve from LSS shown in Fig. 1. The curve above labeled "isotropic α' (12 MeV) emission" is the range-energy curve calculated assuming isotropic (c.m.) emission from the recoil ion of a 12-MeV α. The next curve up, labeled "$F-B$ α' emission" is the range curve calculated assuming the alphas (12 MeV) where emitted 50% forward and 50% backward (0° and 180°). The uppermost curve is the range curve calculated for the emission of two neutrons and a proton subsequent to the α, where all emission is at 0° and 180°. The lowest curve (30-MeV α', $\theta=45°$) is a range curve calculated with the assumption that the α is re-emitted with 30-MeV kinetic energy at a c.m. angle of 45° to the beam.

The influence of nucleon emission was calculated by allowing successive neutron and/or proton emission in the forward and backward directions to follow an initial α-particle emission, also at 0° and 180°. The results of the calculation for the $Ni^{58}(\alpha,\alpha p2n)Co^{55}$ reaction is shown in Fig. 2. Values for other permutations of nucleon emission, which will be shown in subsequent figures, were appropriate. For the $Ni^{58}(\alpha,3pn)Co^{58}$ reaction, the theoretical-range curve was corrected for nucleon emission by allowing the three protons and a neutron to be emitted successively from the recoil ion, each nucleon having a 0°–180° angular distribution. In general, the change in the calculated ranges due to nucleon emission is within the experimental uncertainties of the measured ranges.

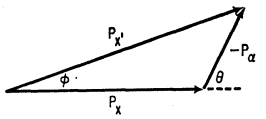

FIG. 3. Vector diagram defining quantities used to calculate ranges following emission of an α with an isotropic angular distribution. The vector $\mathbf{P}_x$ represents the initial recoil momentum of the ion along the beam axis, $-\mathbf{P}_\alpha$ is the change in recoil momentum due to the emission of an α of momentum $\mathbf{P}_\alpha$ at an angle θ with respect to the beam direction, and $\mathbf{P}_x'$ is the resultant ion recoil momentum at an angle φ to the beam direction.

3. *Sensitivity of Range to Symmetry about 90° of the Emitted Alpha Particle*

The preceding discussion indicates that the range is fairly insensitive to the α-particle angular distribution, so long as the angular distribution is symmetric about 90° c.m. A direct interaction would show a predominant forward peaking for the α particle, and so we wish to investigate the sensitivity of the mean recoil range to direct interaction processes. To do this we have taken the entirely arbitrary example of the α particle being emitted at 45° to the beam direction with 30-MeV kinetic energy. The result of this calculation is shown in Fig. 2. If we had assumed a 12-MeV α particle emitted at 45° to the beam, the predicted mean range would be at most 57% of that calculated for a symmetric angular distribution; the great decrease in range is caused not so much by the energy of the emitted α as by the forward peaking. We conclude therefore that the mean recoil range is quite sensitive to the symmetry about 90° c.m. of the emitted particle.

C. Accuracy of Theoretical Range Curves

The authors (LSS) of the range theory we have used have compared available experimental range measurements with their theoretical predictions.[21] Due to the paucity of experimental data in the $\rho-\epsilon$ region of this work, and due to inconsistencies of some of the experimental measurements which are available, it is difficult to state the accuracy of the theoretical curves. We would estimate the curves to be correct to $\pm 10\%$ in the region under discussion in this work. Additional support for the accuracy quoted may be found in results of $Fe^{56}(\alpha,4n)Ni^{56}$, $Fe^{56}(\alpha,3n)Ni^{57}$, $Fe^{56}(\alpha,p2n)Co^{57}$, $Fe^{56}(\alpha,p3n)Co^{56}$, and $Fe^{56}(\alpha,p4n)Co^{55}$ recoil ranges, where the incident helium ion energies varied between 46 and 68 MeV.[23]

A test of interest to the present problem would be a comparison between the experimental ranges of this work which most likely correspond to full momentum transfer and the theoretical ranges. Ranges measured at reaction thresholds must necessarily correspond to full momentum transfer. We have chosen to compare ranges in the region from thresholds to the peaks of

[23] A. Ewart and M. Blann, Bull. Am. Phys. Soc. **9**, 471 (1964).

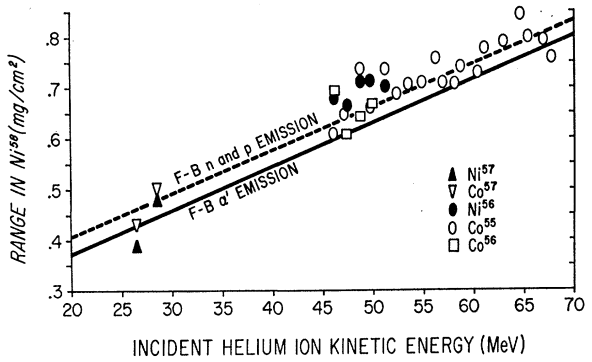

FIG. 4. Comparison of measured recoil ranges from threshold region to excitation function peaks with theoretical ranges. The solid line is the theoretical prediction with α emission at 0° and 180°, the dashed line is the predicted range curve considering the effects of an α, two neutrons and a proton being emitted at 0° and 180°. Triangles represent Ni^{57} ranges, and inverted triangles represent Co^{57} ranges, as measured by Matsuo and Sugihara (Ref. 24). Other points are for the products indicated, and were measured in this work.

excitation functions with the theoretical range curves. In Fig. 4 measured range values are shown with theoretical predictions for Ni^{56}, Ni^{57}, Co^{55}, Co^{56}, and Co^{57} recoils.[24] The agreement is within our estimates of the errors of the recoil range measurements. We conclude from the considerations above that the $\pm 10\%$ estimate of error for the theoretical-range curves is reasonable.

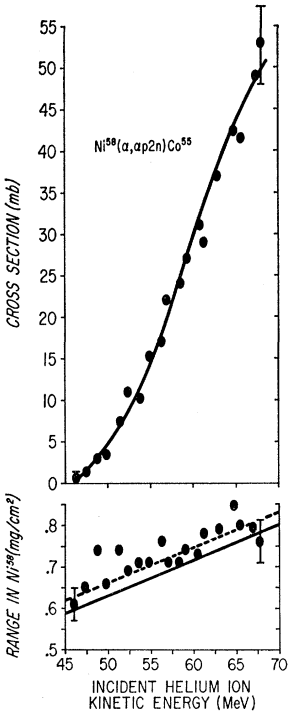

FIG. 5. Excitation function and recoil ranges for $Ni^{58}(\alpha,\alpha p2n)Co^{55}$ reaction. Error flags on the first and last points of the recoil ranges give a visual indication of the estimated accuracy of the points; the flags on the excitation function points are a measure of estimated precision. The solid line on the recoil range graph is the theoretical prediction with correction for α emission at 0° and 180°; the dashed curve has additionally been corrected for evaporation of two neutrons and a proton at 0° and 180°.

IV. RESULTS AND DISCUSSION

This section is divided into two parts. In the first part we shall present the experimental recoil ranges and related excitation functions. We shall discuss the significance of the recoil ranges with respect to momentum transfer in the initial interaction and the angular distribution of the emitted α particles. In the second part we shall speculate on the details of the direct reaction mechanism responsible for the high-energy tails of the Ni^{56}, Ni^{57}, and Co^{57} excitation function.

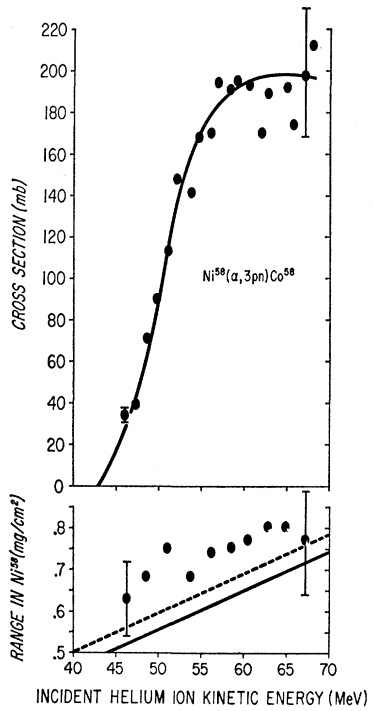

FIG. 6. Excitation function and recoil ranges for $Ni^{58}(\alpha,3pn)Co^{58}$. Error flags on first and last points represent an error estimate for the recoil points, and a precision estimate for the cross sections. The solid curve on the recoil range graph is the theoretical range prediction for the case of no α emission; i.e., the curve from Fig. 1. The dashed curve has been calculated on the assumption that three protons and a neutron have been evaporated from the recoil ion, with a 0°–180° angular distribution.

A. Recoil Ranges and Excitation Functions

Excitation functions for the production of Co^{55} and Co^{58} from Ni^{58}+helium ions are shown in Figs. 5 and 6; the related recoil ranges are also displayed in these figures. The recoil ranges for both reactions are consistent with full momentum transfer from the incident helium-ion beam, implying an α-particle angular distribution which is symmetric about 90° c.m. for the $Ni^{58}(\alpha,\alpha p2n)Co^{55}$ reaction, and symmetry about 90°

[24] The ranges of Ni^{57} and Co^{57} are from results of T. Matsuo and T. T. Sugihara, as reported in Clark University Annual Progress Report (1961), USAEC contract AT (30–1) 1930 (unpublished).

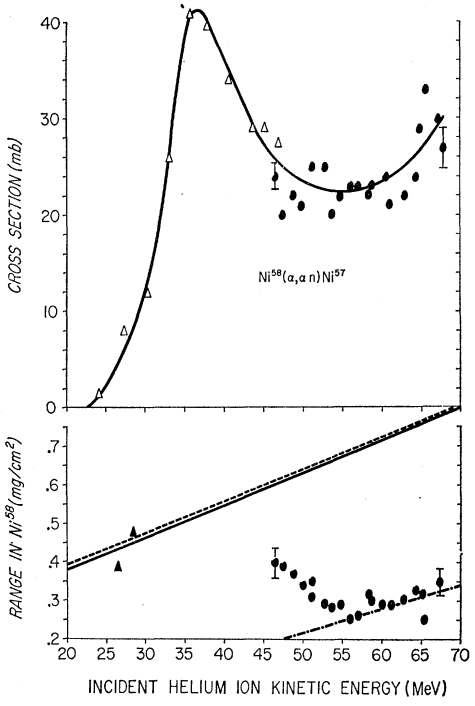

FIG. 7. Excitation function and recoil ranges for the production of Ni^{57} from $Ni^{58}+\alpha$. The cross sections represented by triangles were reported in Ref. 7; the closed triangles on the range graph are due to Matsuo and Sugihara (Ref. 24). Error flags on first and last points (of this work) represent estimates of error in the case of recoil ranges and precision in the case of cross section. The solid curve of the range graph is the theoretical range corrected for evaporation of a 12-MeV α with a 0°–180° angular distribution; the dashed curve also corrects for the evaporation of a neutron with a 0°–180° angular distribution. The dash-dot curve is the range prediction for emission of a 30-MeV α at 45° to the beam; it is included for reference.

c.m. for the nucleons emitted in the $Ni^{58}(\alpha,3pn)Co^{58}$ reaction.

Excitation functions for the production of Ni^{57} and Co^{57} are shown in Figs. 7 and 8, as are the related recoil ranges. For both products the recoil ranges near threshold are consistent with full momentum transfer. The next recoil values available are for the reactions induced with 46-MeV helium ions. At this point the excitation functions have passed their maxima and have started into a high-energy tail. The recoil range for Co^{57} at this point indicates that full momentum transfer persists, but adjacent values indicate that the momentum transfer is rapidly decreasing, as the tail becomes more pronounced. We believe it is safe to assume that full momentum transfer persists in the production of Co^{57} between 28- and 46-MeV incident helium-ion energy, since recoil ranges at 28 and 46 MeV show full momentum transfer. In the case of the Ni^{57} recoil range at 46 MeV, momentum transfer is significantly less than complete, and decreases rapidly with increasing incident helium-ion energy. The peak of the $Ni^{58}(\alpha,\alpha n)Ni^{57}$ excitation function may result therefore from both compound nucleus and direct interaction contributions: The sum of these must be greater than the compound nucleus contribution alone. It may be concluded therefore that the low yield of Ni^{57} with respect to Co^{57} at the excitation function peaks may not be attributed to an (α,α') direct reaction mechanism, but is rather a property of the decay of the compound nucleus. The effect of the 28-nucleon shell on level densities may be the explanation for the low Ni^{57} yields.[7,25–27]

It may also be concluded from Figs. 7 and 8 that the preponderate reactions leading to the excitation function tails of Co^{57} and Ni^{57} are low momentum transfer or "direct" reactions, in which the emitted α particle is peaked forward. In part B of this section we shall discuss the direct reaction mechanism in greater detail.

At the highest energies studied in this work, the excitation functions for the production of Co^{57} and

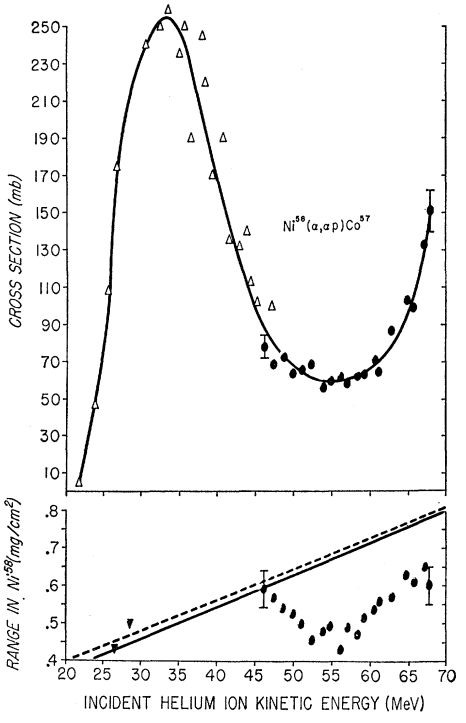

FIG. 8. Excitation function and recoil ranges for the production of Co^{57} from $Ni^{58}+\alpha$. The cross sections represented by triangles were reported in Ref. 7; the inverted triangles on the range graph are due to Matsuo and Sugihara (Ref. 24). Error flags on the first and last points (of this work) represent estimates of error in the case of recoil ranges, and of precision in the case of cross sections. The solid curve of the range graph is the theoretical range corrected for evaporation of a 12-MeV α with a 0°–180° angular distribution; the dashed curve also corrects for the evaporation of a neutron with a 0°–180° angular distribution.

[25] C. Bloch, Phys. Rev. **93**, 1086 (1964).
[26] N. Rosenzweig, Phys. Rev. **108**, 817 (1957).
[27] R. A. Sharp, R. M. Diamond, and G. Wilkinson, Phys. Rev. **101**, 1493 (1956).

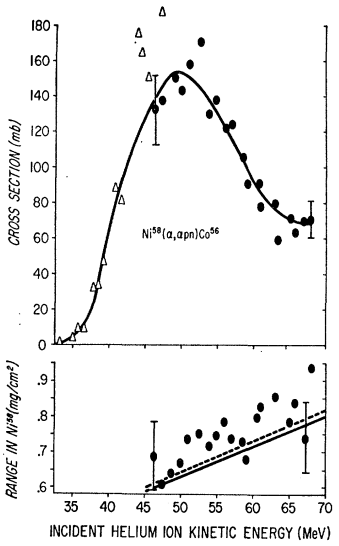

FIG. 9. Excitation function and recoil ranges for the $Ni^{58}(\alpha,\alpha pn)Co^{56}$ reaction. Cross sections represented by triangles were reported in Ref. 7. Error flags on the first and last points of the recoil ranges and cross sections represent an estimate of accuracy and precision, respectively. The solid line on the range curve is the theoretical value corrected for 0°–180° α emission; the dashed curve has additionally been corrected for the emission of a p and an n with a 0°–180° angular distribution.

Ni^{57} start to show a rapid increase which is also reflected by an increase in recoil range. This feature probably corresponds to the onset of the $Ni^{58}(\alpha,3p2n)Co^{57}$ and $Ni^{58}(\alpha,2p3n)Ni^{57}$ compound nucleus reactions, which is consistent with the predictions of the statistical model.[8]

The excitation function for the $Ni^{58}(\alpha,\alpha pn)Co^{56}$ reaction with the associated recoil ranges is shown in Fig. 9. The excitation function exhibits a high-energy tail, which apparently results from reactions with full momentum transfer. A consideration of possible experimental errors, notably photopeak integration of the catcher-foil γ-ray spectra, leads us to estimate a maximum of 30% low-momentum transfer component in the excitation-function tail. Thus, the preponderance of reactions leading to Co^{56} in this region ($E_\alpha \approx 60$–68 MeV) may not be attributed to a direct interaction, but must be ascribed to a compound-nucleus mechanism. The failure of a statistical theory calculation (with an assumed $2J+1$ spin distribution) to reproduce this tail must, therefore, be ascribed to a failure of the theory in the form in which it has been applied, rather than to a direct reaction mechanism.

A probable explanation for the compound-nucleus tail is that it results from γ-ray de-excitation successfully competing with emission of a fourth particle. The rationale for this explanation in terms of high-angular momentum of the "cool" nucleus (prior to emission of the last particle), spin states available near ground, and the angular momentum an evaporated particle may remove, has been given elsewhere.[28] An optical-model calculation indicates angular momentum contributions from $l \approx 23\hbar$ are significant at the highest bombarding energies of this work.[8] The Co^{56} excitation-function tail may represent the decay of compound nuclei formed with the higher angular momenta of the total spin distribution. If this were the case, the failure of the statistical theory may be ascribed to the failure to include a satisfactory estimate of γ-ray nucleon-emission competition. An alternative explanation for the compound nucleus tail would be particle evaporation prior to the establishment of statistical equilibrium. Both explanations could be valid, although simple considerations of single particle versus collective motion make the latter explanation seem the less likely. The present experiments do not permit a definite conclusion to be reached.

We wish to emphasize that the high-energy tail of the Co^{56} excitation function does result preponderately from a full momentum-transfer reaction; there is, therefore, a significant amount of physical information on compound-nucleus theory available in the tail of this and other excitation functions where full momentum transfer has been shown to exist.[23] Thus, that part of the excitation function which has too often been lightly dismissed as being due to a direct interaction should be scrutinized more closely for information which particle spectral measurement cannot yet give. For example, if the first explanation of the previous paragraph were correct, the tail of the Co^{56} excitation function combined with the Co^{55} and Fe^{55} excitation functions might be used to study the difference in decay properties of compound nuclei at the same excitation but of different angular momenta. Compound-nucleus excitation-function tails might also be used to estimate the angular momentum cutoff for incident ions, i.e., at approximately what impact parameter incident ions of a given mass and energy cease to form compound nuclei and start to react predominantly at the nuclear surface. This information in turn would be valuable in the calculation of inverse-reaction cross sections.

The excitation function and related recoil ranges for the $Ni^{58}(\alpha,\alpha 2n)Ni^{56}$ reaction are presented in Fig. 10. The recoil ranges show a full momentum transfer approximately up to the peak of the excitation function, after which the momentum transfer steadily decreases as the incident helium-ion energy increases. The decrease in momentum transfer to the recoil ions is accompanied by an increase in reaction cross section, indicating a competing low-momentum transfer process is becoming increasingly significant.

B. Direct Reaction Mechanisms

We have shown (part A of this section) that the high-energy tails of the Ni^{57}, Co^{57}, and Ni^{56} excitation functions result predominantly from low-momentum transfer reactions in which the α particle is emitted in the forward direction. The two most likely mechanisms

[28] R. Grover, Phys. Rev. **123**, 267 (1961).

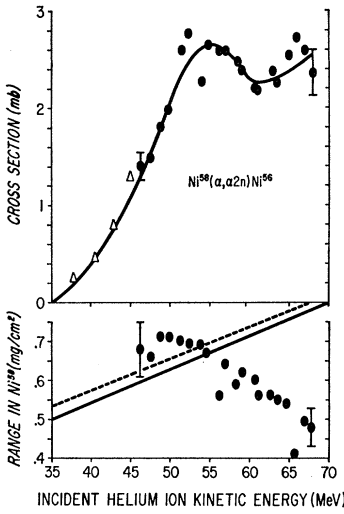

FIG. 10. Excitation function and recoil ranges for the $Ni^{58}(\alpha,\alpha 2n)Ni^{56}$ reaction. Cross sections represented by triangles were reported in Ref. 7. Error flags on the first and last points of the recoil ranges and cross sections represent an estimate of accuracy and precision, respectively. The solid line on the range curve is the theoretical value corrected for 0°–180° α emission; the dashed curve has additionally been corrected for the emission of two neutrons with a 0°–180° angular distribution.

for these reactions are an initial interaction between the incident helium ion and a nucleon (or nucleons) of the nucleus, with the helium ion and nucleon (or nucleons) involved being ejected directly, or alternatively an inelastic scattering of the incident helium ions followed by nucleon evaporation from some spectrum of excited Ni^{58} nuclei. Some combination of the latter mechanisms could of course also be present. If the (α,α') inelastic-scattering+nucleon-evaporation mechanism were the predominant contributor to the reactions under discussion, then we would expect the ratios $\sigma Co^{57}/\sigma Ni^{57}$ and $\sigma Co^{56}/\sigma Ni^{56}$ in the excitation-function tails to be some combination of the ratios resulting from the decay of Ni^{58} compound nuclei at a spectrum of excitation energies. Houck and Miller have measured the $Fe^{54}(\alpha,p)Co^{57}$, $Fe^{54}(\alpha,n)Ni^{57}$, $Fe^{54}(\alpha,pn)Co^{57}$ and $Fe^{54}(\alpha,2n)Ni^{56}$ excitation functions with 7- to 39-MeV helium ions.[5] We shall use these excitation functions to evaluate the yield ratios discussed above (thus, we are assuming that the reactions of $Fe^{54}+\alpha$ proceed by a compound-nucleus mechanism).

The ratio $\sigma Co^{57}/\sigma Ni^{57}$ from the reaction $Fe^{54}+\alpha$ varies between 2:1 and 4:1. The corresponding ratio in the excitation-function tails of this work is 3:1. While this is consistent with the decay of some spectrum of excitations of Ni^{58}, it is not necessarily inconsistent with a direct (α, nucleon) interaction. We therefore cannot differentiate between the two proposed mechanisms for the Co^{57} and Ni^{57} excitation function tails.

The ratio $\sigma Co^{56}/\sigma Ni^{56}$ resulting from the helium-ion bombardment of Fe^{54} varies between 100:1 and 48:1 in the excitation interval between 28 and 45 MeV. Based on this information we would predict that if the 2.5-mb Ni^{56} cross section (for 68-MeV incident helium-ion energy) were due to decay of Ni^{58} nuclei, then the yield of Co^{56} from the same inelastic α-scattering process would be at least 125 mb. In Fig. 9 it may be seen that the corresponding yield of Co^{56} is 70 mb, and the preponderate part of this yield results from a full momentum transfer process rather than from a low-momentum transfer process. While it is correct that not all the Ni^{56} yield (at 68-MeV He^{++} energy) need necessarily have resulted from the low-momentum transfer process, the major portion did. We cannot, therefore, find consistency with the $Fe^{54}(\alpha,2n)$ and $Fe^{54}(\alpha,pn)$ results by postulating a $Ni^{58}(\alpha,\alpha')Ni^{58*}$ +nucleon evaporation mechanism. This interpretation would suggest a direct (α, neutron) or (α, two neutron) reaction mechanism. We present this argument more in the spirit of speculation than as a conclusion. It may be significant that the target nucleus consists of a closed proton shell and two neutrons outside a closed neutron shell.

V. CONCLUSIONS

The theoretical range-energy curves for heavy ions due to Lindhard *et al.*[21] provide a useful tool for the interpretation of recoil measurements. We have compared some of the experimentally measured ranges of this work with theoretical curves corrected for the effect of particle evaporation. The ranges which have been compared with theory correspond to points on the excitation functions between threshold and maxima; agreement is to within 10%. The recoil ranges in this region are quite sensitive to symmetry about 90° of emitted α particles, and therefore are a useful tool in gaining this information on the α-particle angular distribution.

Since the peak of the Co^{57} excitation function is apparently due to a compound-nucleus mechanism, the low yield of Ni^{57} must be explained in terms of the compound nucleus-reaction mechanism. It has been suggested that the low yield results from the influence of the 28-nucleon shell on level densities.[7,25–27] Low-momentum transfer reactions account for the preponderance of reactions producing Ni^{57} and Co^{57} in the region of the high-energy tails of the excitation functions, implying that the emitted α particles are peaked in the forward direction. At the highest energies studied in this work, both excitation functions and recoil ranges show an increase consistent with the onset of the $Ni^{58}(\alpha,3p2n)Co^{57}$ and $Ni^{58}(\alpha,2p3n)Ni^{57}$ compound nucleus reactions.

The $Ni^{58}(\alpha,\alpha p2n)Co^{55}$ and $Ni^{58}(\alpha,3pn)Co^{58}$ reactions appear to be proceeding by a compound-nucleus mechanism over the excitations studied in this work. The $Ni^{58}(\alpha,\alpha pn)Co^{56}$ recoil ranges are also consistent with a full momentum transfer over the entire energy range studied, including the values corresponding to the high-energy tail of the excitation function. As in the

case of the Ni^{57}/Co^{57} ratios at the excitation-function peaks, we conclude that the anomalously low yields of Ni^{56} with respect to Co^{56} must be explained within the framework of the compound-nucleus reaction model, rather than as a direct process. As with the $Ni^{57}-Co^{57}$ excitation functions, we suggest a probable explanation of low Ni^{56} yields is a decrease in level densities for the 28-nucleon closed shell.

The $Ni^{58}(\alpha,\alpha 2n)Ni^{56}$ recoil ranges are consistent with a compound-nucleus mechanism up to the peak of the excitation function; beyond this point there is an increasing contribution from a low-momentum transfer reaction mechanism, accompanied by an increase in cross section at the highest energies studied. We feel that this data, when compared with $Fe^{54}(\alpha,2n)Ni^{56}$ and $Fe^{54}(\alpha,pn)Co^{56}$ excitation functions, implies that the direct process in question is between the incident helium ion and one or both neutrons, rather than an (α,α') inelastic scattering process followed by nucleon evaporation.

ACKNOWLEDGMENTS

We are grateful to Herman Grunder and the crew of the Lawrence Radiation Laboratory 88-in. cyclotron for the bombardments of this work, and to the Chemistry Division of the Lawrence Radiation Laboratory for permitting us to use the facility while one of the authors (M.B.) was a visitor at the laboratory. We sincerely appreciate the permission given by Professor T. T. Sugihara to quote his and Dr. Matsuo's unpublished results, and we appreciate helpful discussions with Professor Sugihara as well. We are grateful for additional thought provoking discussions in the course of this work with Professor J. M. Alexander, Professor J. M. Miller, and Dr. G. Merkel. Our thanks to L. Schwartz and J. Cooper for the drawings used in this work. We are grateful to Professor J. M. Alexander for a critical review of this manuscript. We appreciate the help of Mrs. R. Lorimer in setting up equipment for the helium-ion bombardments.

PHYSICAL REVIEW VOLUME 134, NUMBER 4B 25 MAY 1964

Differential Cross Sections for the Reaction $C^{13}(Li^6,\alpha)N^{15}$†

J. M. Blair, Pham-Dinh-Lien, and Russell K. Hobbie
School of Physics, University of Minnesota, Minneapolis, Minnesota

(Received 3 January 1964)

Differential cross sections have been measured for the reaction $C^{13}(Li^6,\alpha)N^{15}$ with the residual nucleus in its ground and first two excited states, the bombarding energy ranging from 3.4 to 4.0 MeV. They have general features suggesting a direct interaction.

INTRODUCTION AND PROCEDURE

To further the investigation of reactions induced in light nuclei by Li ions,[1–4] we have measured the differential cross sections for the reaction $C^{13}(Li^6,\alpha)N^{15}+14.69$ MeV.

The equipment for producing the beam of Li ions has been described in an earlier paper.[1] The target chamber has been designed by Pinsonneault for studying the elastic scattering Li on Li.[5]

The carbon target was made by cracking methyl iodide onto a 5×10^{-6}-in. thick nickel foil.[6] By varying the heating time and the pressure of the methyl iodide vapor, targets with different thicknesses were obtained. The target used in this experiment was produced using a pressure of 10 Torr and a heating time of 4 sec. The total thickness of the target when traversed at an angle of 45° was 380±30 keV for 3.6-MeV Li^6 ions.

Alpha particles from the reaction stopped in a silicon-junction detector whose amplified output was displayed on a 512-channel pulse-height analyzer. The angular width of the detector as seen from the target was 0.4°.

Angular distributions were measured at laboratory angles from 20° to 160° in 10° steps, for bombarding energies of 3.4, 3.6, 3.8, and 4.0 MeV.

The total number of C^{13} and C^{12} target nuclei was obtained from the yield of Li ions which underwent Rutherford scattering from carbon. The number of C^{12} nuclei in the target was determined from the yield of α particles from the reaction $C^{12}(Li^7,\alpha)N^{15}$, whose cross section is known.[3] By comparing these we found that the carbon in the target contained (52±13%) C^{13}. Absolute cross sections were determined by comparing the yield of α particles from the reaction $C^{13}(Li^6,\alpha)N^{15}$ with that of Li ions scattered elastically by the target nuclei.

RESULTS

We have corrected the energy by using the average energy $E_0=E_{\text{machine}}-\Delta E$, where $2\Delta E$ is the energy lost

† This work was supported in part by the U. S. Office of Naval Research.

[1] J. J. Leigh and J. M. Blair, Phys. Rev. **121**, 246 (1961).
[2] R. K. Hobbie, C. W. Lewis, and J. M. Blair, Phys. Rev. **124**, 1506 (1961).
[3] R. K. Hobbie and F. F. Forbes, Phys. Rev. **126**, 2137 (1962).
[4] J. M. Blair and R. K. Hobbie, Phys. Rev. **128**, 2282 (1962).
[5] L. L. Pinsonneault, Ph.D. thesis, 1964, University of Minnesota (unpublished).
[6] H. D. Holmgren, J. M. Blair, K. F. Famularo, T. F. Stratton, and R. V. Stuart, Rev. Sci. Instr. **25**, 1026 (1954).